CrystEngComm

Accepted Manuscript

ROYAL SOCIETY OF CHEMISTRY

www.rsc.org/crystengcomm

CrystEngcomm CrystEngComm

Cite this: DOI: 10.1039/c0xx00000x

www.rsc.org/xxxxxx

ARTICLE TYPE

Dynamically controlled synthesis of different ZnO nanostructures by surfactant-free hydrothermal method

Haili Li,[a] Shujie Jiao,*[a,b,c] Shiyong Gao,*[a] Hongtao Li[a] and Lin Li[b]

Received (in XXX, XXX) Xth XXXXXXXXX 20XX, Accepted Xth XXXXXXXXX 20XX

DOI: 10.1039/b000000x

To broaden the device applications of ZnO nanomaterials, various ZnO nanostructures are fabricated by a "green" hydrothermal method. To achieve the dynamically controlled surfactant-free hydrothermal growth of ZnO, the nutrient solutions of zinc acetate dihydrate and hexamine are stirred or aged for some certain time beforehand. X-ray absorption fine structure analysis of intermediates in disturbed solutions indicates that the coordination number of Zn atoms varies with different pretreatments. The Zn-O bond length, which is sensitive to both the coordination numbers of Zn and the amount of atoms consisted in each agglomerates, also shows different values. Based on the fact that the total amount of Zn^{2+} in each nutrient solution is constant, the formation of different ZnO nanostructures evolution from ZnO nanorods to nanotapers and rod-on-nanorod structure can then be designed and understood from the standpoint of dynamic by using agglomerates with different sizes and concentrations as building blocks. Particularly, ZnO nanopencils with high crystallinity and optical properties are obtained by this method. This rational engineering of building blocks in solutions provides not only a fundamental research on the effects of physical disturbances on the structure of agglomerates and final ZnO products, it also promises a new idea for tunable and "green" fabrications of versatile ZnO nanostructures with the assistance of external force.

INTRODUCTION

In recent years, ZnO has attracted enormous attention due to its advantageous characteristics of wide band gap (3.37 eV), large exciton energy (60 meV) and piezoelectric property for applications in various fields.[1-3] Besides, ZnO is also capable of engineering different morphologies into devices,[4-7] especially for ZnO nanomaterials with sharp tips, which possess thermal stability and oxide resistibility characteristics of ZnO, as well as the advantages of lower turn-on field, high emission rate of electron and fast electron-transfer rate properties.[8,9] Even though many methods are feasible for fabrications of different ZnO nanomaterials,[10-12] high temperature, surfactants, or complex procedures are needed in most cases. In comparison, hydrothermal method is a good choice in term of its low cost, mild growth conditions, eco-friendly properties and enormous efforts have been devoted to explore the effect of surfactants,[13] concentrations,[14] time[15] on morphologies. As a result of rapid developments in synthetic methods, the prefabricated component from physical or mechanistic process before hydrothermal as building blocks are of great significance for "green" fabrications and applications of ZnO. But reports on this issue are much less.[16,17] For a better understanding of the controllable organization and growth mechanism, more fundamental explorations from micro perspective are urgently needed.

In this article, dynamically controlled growth of different ZnO nanostructures is achieved by exerting different stirring and aging treatments to the reaction solutions before hydrothermal growth. The effects of physical disturbance on the morphology and properties of final ZnO nanomaterials are studied in detail. Most importantly, the atomic mechanism for the formation of versatile ZnO nanostructures in disturbed solutions is also explored by X-ray absorption fine structure characterization.

MATERIALS AND METHODS

Chemical and materials

Zinc acetate dihydrate ($Zn(AC)_2{\cdot}2H_2O$, 99.0%), Hexamine (HMT, 99.0%), Ethanol (C_2H_5OH, 99.9%) and Lithium hydroxide monohydrate ($LiOH{\cdot}H_2O$) were obtained from Samchun. All reactants were used as received, without further purification. Indium tin oxide (ITO) substrate was obtained from Nanbo Company and deionized water was obtained by using a DBW Water Purification Machine (DBW-SYS).

Preparation of different ZnO nanostructures

A sealed hydrothermal growth environment was used to fabricate different ZnO nanostructures at low temperature. The nutrient solutions for hydrothermal growth of ZnO were formed by pouring $Zn(AC)_2{\cdot}2H_2O$ aqueous into HMT aqueous solution. For dynamic controlled synthesis of ZnO at nanoscale, the as-synthesized solutions were treated in different ways before hydrothermal growth. In detail, the three different pre-treatments exerted to the nutrient solutions can be described as follows: (a) Stirring for 5 min (T0); (b) Stirring for 3 h (T1); (c) Stirring for 3 h and aged for another 21 h (T2). In a typical hydrothermal growth process of ZnO nanomaterials, ZnO seed layer was firstly formed on ITO substrate by sol-gel based dip coating method as mentioned before.[18] In brief, clean ITO substrate was immersed in the sol-gel solution for 30 min before being pulled out at the rate of 0.5 cm/min and dried at room temperature. Secondly, hydrothermal growth of ZnO formed on substrate was performed

in the teflon-lined pressure vessel at 90 °C. Taking the effect of gravity into consideration, the substrate coated with ZnO seed layer was suspended in the solution with its conductive side down. After reaction, the reactor was put into the cold water bath (20 °C) immediately and kept for 1 min. Eventually, the sample was picked out and dried at room temperature for 30 min after being rinsed with deionized water thoroughly. The effects of nutrients concentrations on the structure of ZnO nanomaterials were studied by using solutions treated in T2 way.

Characterization

Morphology and structure characterizations of the as-synthesized ZnO nanostructures were measured by Scanning electron microscope (KYKY-EM6000C, 20 KV) and X-ray diffractometer (Panalytical's X-ray diffractometer, 20 mA, 50 KV) with $Cu_{k\alpha}$ radiation. Photoluminescence spectra were recorded at room temperature with excitation wavelength of 325 nm (He-Cd laser). For a structural characterization of zinc complexes formed in solutions with different pretreatments, X-ray absorption fine structure characterization (XAFS) was conducted at the XAFS station of the 1W1B beamline of the Beijing Synchrotron Radiation Facility (BSRF). Aqueous samples were injected into the sample cells. Zn K-edge EXAFS spectra were collected at room temperature in transmission or fluorescence mode. Samples with very low concentration were measured by elements solid-state detector. The storage ring was working at 2.5 GeV with a maximum electron current of about 250 mA. Data were collected using a Si (111) double-crystal monochromator and analyzed using the IFEFFIT program.

Results and discussion

Morphology control via pretreatments to solutions

Fig. 1 shows the SEM micrographs of ZnO nanomaterials synthesized with solutions treated in T0, T1 and T2 way. All samples in this section were synthesized by hydrothermal method at 90 °C for 3h. Even though $Zn(AC)_2{\cdot}2H_2O$ (0.03 M) and HMT (0.06 M) are commonly used for fabrications of ZnO nanorods, with different physical disturbances done to the nutrient solutions, the as-synthesized samples shown in Fig. 1a-1c illustrate remarkably different morphologies. With the solution in Fig.1a treated in T0 way, high density ZnO nanorods with diameters 55 nm were formed, which is in good accordance with the previous results.[19] Interestingly, when solution was treated in T1 way, as presented in Fig.1b, tapered ZnO nanostructure with diameter decreasing from the base to the top was obtained. Compared with nanorods in Fig. 1a, the average diameter of the top part of ZnO nanotapers increased to 300 nm. Fig. 1c shows the SEM micrograph of the sample formed with solution treated in T2 way. The as-synthesized sample exhibits coaxial-cable ZnO nanostructure. Each cable is composed of a big rod with diameter 420 nm and a smaller rod with diameter 170 nm grown on the top. Both rods are in typical hexagonal structures. Judging from these experimental results, it is reasonable to be believed that different pretreatments to precursors are crucial for fabrications of different ZnO nanostructures.

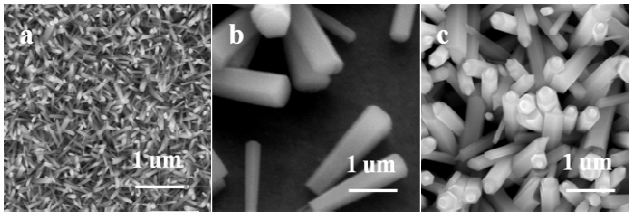

Fig. 1 SEM images of ZnO nanostructures grown using solutions with a) T0; b) T1; c) T2 pretreatment.

Effects of concentrations of reactants in disturbed solution on the structure of ZnO

SEM images of ZnO nanomaterials synthesized in T2-way treated solutions with different concentrations are illustrated in Fig. 2. All growth processes in this section were performed at 90 °C with growth time 4.75 h. The concentrations of $Zn(AC)_2{\cdot}2H_2O$ and HMT in Fig. 2a were 0.03 M and 0.03 M and ZnO nanorods with blunt tips 125 nm were formed. When the concentration of HMT increased to 0.06 M, as presented in Fig. 2b, ZnO nanopencils with sharp tips capping on the hexagonal stem were synthesized. The average diameter for the top part of the hexagonal stem is 70 nm. As illustrated in Fig. 2c, low density rod-on-nanorod ZnO nanomaterial was formed when both the concentrations of the two reactants increase to 0.06 M. Besides, the size of the products in Fig. 2a -2c also increased with concentrations.

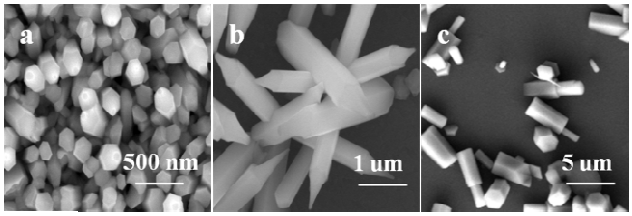

Fig. 2 SEM images of ZnO nanostructures grown in T2-way treated solutions with concentrations of HMT and $Zn(AC)_2$: a) 0.03 M+0.03M; b) 0.03 M+0.06M; c) 0.06 M+0.06M.

Crystallinity and optical properties of ZnO nanopencils

Fig. 3 is the XRD characterization result of the as-synthesized samples. The curves in Fig. 3 belong to ZnO nanorods and nanopencils mentioned in Fig. 1a and Fig. 2b, respectively. All peaks can be well indexed to wurtzite hexagonal phase of ZnO (JCPDS 36-1451, a=0.325 nm, c=0.521 nm)[20] and ITO substrate (as indicated by solid squares), no impurity phases are observed. The sharp and strong peaks indicate that both samples are in good crystallinity. The X-ray diffraction result of ZnO nanopencil is in good accordance with reference 21. For a better description of their orientation properties, texture coefficient (*TC*) is introduced as shown in Eq. (1).[22]

$$TC\,(hkl) = \frac{\frac{I(hkl)}{I_0(hkl)}}{\sum_n \frac{I(hkl)}{I_0(hkl)}} \times 100\% \qquad (1)$$

Where I (hkl) and I_0 (hkl) are the measured and standard intensity of plane (hkl) taken from the JCPDS data. It is commonly accepted that higher *TC* value indicates that nanomaterials are oriented in a given (hkl) direction. Consequently, the higher *TC (002)* value for sample synthesized with solutions treated in T1

way indicates that ZnO nanorods with c-axial growth direction are highly aligned perpendicular to the substrate. As for the situation for ZnO nanopencils shown in Fig. 2b, a lower *TC (002)* value is obtained, which is in good accordance with the random distribution of ZnO nanopencils shown in Fig. 2b. [23] Optical properties, as a useful method to characterize the defects and impurities in materials, are of great value for their technique applications. The optical properties of the as-synthesized ZnO nanorods and nanopencils shown in Fig. 4 are investigated by room temperature photoluminescence spectroscopy. The UV emissions with wavelength 380 nm shown in both samples in Fig. 4 are well accepted as the near-band-edge emission, which can be attributed to the recombination of free excitons.[24] Even though the visible emission band induced by the defects is usually observed for most ZnO nanomaterials,[25,26] herein, only strong near-band edge UV emissions are observed, which indicates that ZnO nanomaterials with high optical quality are successfully achieved. Additionally, the high intensity near-band-edge emission also illustrates that the as-synthesized ZnO sample is in high crystallinity, which makes it a good candidate of light emission device.[27]

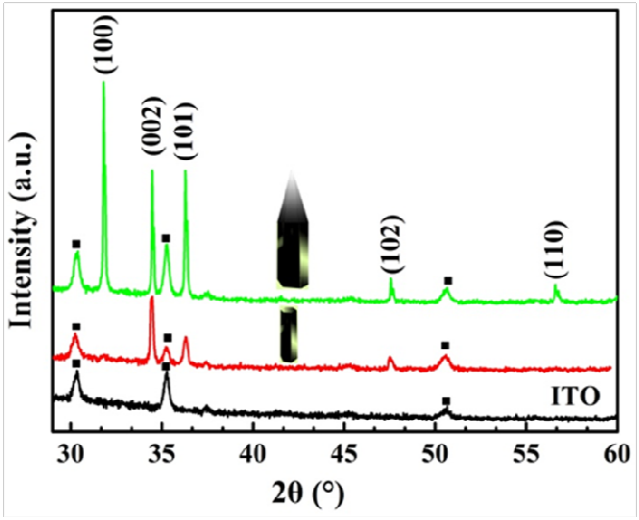

Fig. 3 XRD spectra of ZnO nanopencils and nanorods.

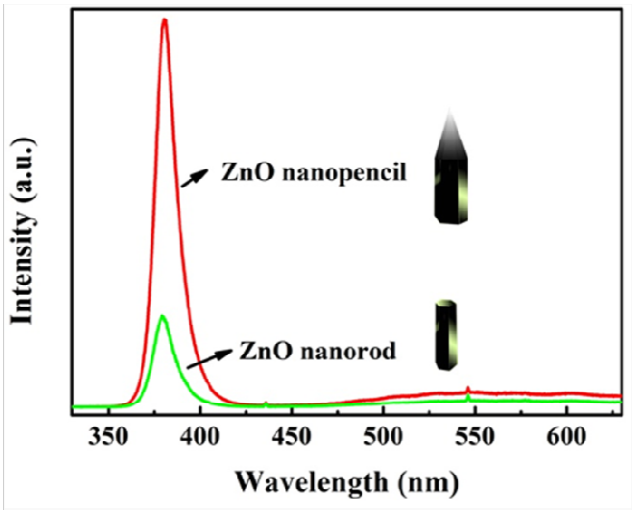

Fig. 4 PL spectra of ZnO nanopencils and nanorods.

Mechanism

Generally, hydrothermal growth of ZnO nanomaterials with $Zn(OH)_2$, $Zn(OH)_4^{2-}$ as growth units [28,29] follows the reaction processes shown in Eqs. (2)-(7).[30-32] The use of $Zn(AC)_2{\cdot}2H_2O$ (0.03 M) and HMT (0.06 M) is generally resulted in the formation of ZnO nanorods. Herein, by exerting physical disturbance to reaction solutions, different ZnO nanostructures were formed. The pH detection of solutions indicates that their pH values slightly decrease with T0, T1 and T2 treatments from 6.65 to 6.4 and 6.31. These variations indicate that the solution characteristic changed with different physical disturbances. Referring to the atomistic simulations of ZnO aggregation performed by Agnieszka Kawska, et al, aggregations in the form of $Zn_x(OH)_y]^{(2x-y)+}$ formed and changed in both the size and combination configure through proton transfer.[33] Thus, it is reasonable to deduce that the coordination number of Zn and the amounts of atoms consisted in each agglomerates may be changed by being provided with extra energy and time through T1 and T2 pretreatments to solutions.

$$Zn(CH_3COO)_2 \leftrightarrow Zn^{2+} + 2CH_3COO^- \quad (2)$$

$$(CH_2)_6N_4 + 6H_2O \rightarrow 6HCHO + 4NH_3 \quad (3)$$

$$Zn^{2+} + 4NH_3 \leftrightarrow Zn(NH_3)_4^{2+} \quad (4)$$

$$Zn^{2+} + 4OH^- \leftrightarrow Zn(OH)_4^{2-} \rightarrow ZnO + H_2O + 2OH^- \quad (5)$$

$$Zn^{2+} + 2OH^- \rightarrow Zn(OH)_2 \rightarrow ZnO + 2H_2O \quad (6)$$

$$Zn(NH_3)_4^{2+} + 2OH^- \rightarrow ZnO + 4NH_3 + 2H_2O \quad (7)$$

To confirm the formation of agglomerates and further explore the effects of stirring and aging processes on these zinc intermediates, XAFS test result is given in Fig. 5. The curves were not treated with phase shift correction. Fig. 5a is the X-ray absorption coefficients of samples near the Zn K edge. Fig. 5b and its inset curve are the Fourier transformed R-space XAFS results of the agglomerates in different disturbed solutions and standard ZnO. In Fig. 5a, all samples show high absorptions at the characteristic energy absorption for Zn K-edge (at about 9659 eV). While in Fig. 5b, the R-space curves of intermediates show different peak positions and wider peak width from standard ZnO, which confirms the formation of zinc intermediates. For a specific exploration, all sets of the XAFS data Fourier transformed to R-space were fitted to the theoretical XAFS calculations, as shown by the dash lines in Fig. 5b. The quick first shell fit results with the R-rang 1-4 Å are summarized in Table 1. σ^2 is Debye-Waller factors for disorder. The judgment parameter of goodness of the fitting (R_{factor}) is far below 0.02. The coordination number (CN) presents the numbers of neighbours of Zn atoms and bond distance (R) mentioned here is the distance between Zn atoms and their neighbours in agglomerates.[34] Generally, six-coordinated octahedron geometry and four-coordinated tetrahedron are two typical coordination configurations for zinc complexes. In this article, the fitting CN value of Zn in solutions with T0 treatments is 5.4, which indicates that these zinc intermediates should be mainly in octahedral coordination by combination between Zn^{2+} and 6 H_2O.[35] As the crystal structure of these agglomerates is more open than ZnO, dehydration process takes place between every two nearest hydroxyl groups. The resulting H_2O molecule was loosely affiliated to aggregate and eventually diffused into the solvent.[38] While O^{2-} ions remains in the aggregate and prompts the structural rearrangement.[33] By further providing agglomerates with external energy and time through stirring and aging processes of solutions, it is reasonable to believe that some parts

in agglomerates transformed from octahedral combination to tetrahedral coordination during the T1 or T2 processes, which well explains the decreasing CN values of agglomerates in solutions with T1 and T2 treatments from 5.2 to 4.8. These transformations give closer values of the coordination number of Zn in wurtzite ZnO structure. Besides, the Zn-O bond length, which is sensitive to its surrounding environments, is a key parameter for detecting variations in agglomerates. It is reported that increase in the amounts of atoms in agglomerates may enlarge the bond length.[36] While it is well-known that transformation from octahedron coordination to tetrahedron coordination shall lead to a decreasing bond length as the characteristic Zn-O bond length for tetrahedral combination is about 0.1 Å shorter than the Zn-O distance for octahedral coordination.[37] The bond length in this article shall then be determined by the competition of these two processes. As shown in Table 1, the bond length of agglomerates formed in solutions with T0, T1 pretreatments firstly increased from 2.08 Å to 2.089 Å, which can be attributed to the increase in the amount of atoms consisted in each agglomerates. By further aging the solution for another 21 h, the bond length decreased from 2.089 Å to 2.082 Å indicating that transformation from octahedron coordination to tetrahedron coordination domains this process, which is in good accordance with the substantially declination in the coordination number of Zn from 5.2 to 4.8.

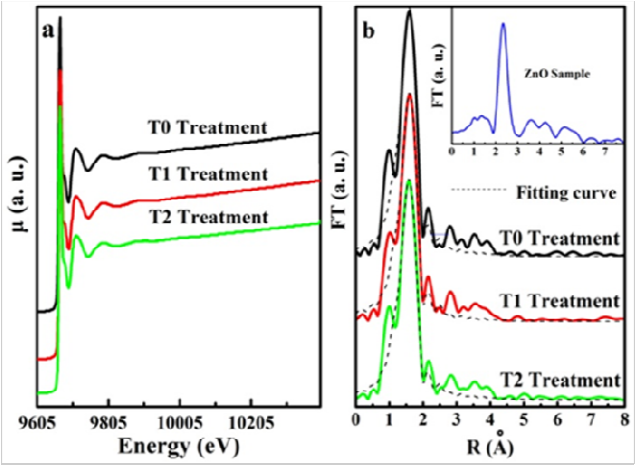

Fig. 5 XAFS characterization of intermediates formed in solutions with T0, T1 and T2 treatment: a) X-ray absorption coefficients of at Zn K edge measured as a function of the incident X-ray energy; b) are magnitude of Fourier transformed XAFS as a function of the distance from a Zn atom and the corresponding fitting curves.

Table 1 First shell fitting results of different agglomerates formed in disturbed solutions.

Samples	Bond	CN	R/ Å	σ^2	R_{factor}
0	Zn-O	5.40	2.080	0.00081	0.000180
1	Zn-O	5.20	2.089	0.00786	0.000150
2	Zn-O	4.80	2.082	0.00913	0.000210

All these experimental results indicates that the size enlargement of agglomerates mainly happened in the stirring process of solutions and the aging process of solutions prompts the transformation of agglomerates from octahedron combination to tetrahedron combination greatly. As the total amount of Zn^{2+} in each solution is constant, the concentrations of agglomerates shall be in reverse relationship with the number of atoms consisted in agglomerates. That is to say, the concentration of agglomerate in the disturbed solution decreases with its size. Together with the fact that the growth rates of different facets, which determine the final morphology of ZnO, are in close relationship with variations in the size and concentration of building blocks. Fabrications of different ZnO nanomaterials in this article can then be understood from dynamic way. The schematic diagram is illustrated in Fig.6. The nutrient solutions in the green, blue and purple beakers in Fig. 6a are treated in T0, T1 and T2 way, respectively. As shown in Fig. 6a-i, six-coordinated agglomerates with small size and large quantity are formed in the solution with T0 treatment. According to crystallography, agglomerates tend to adsorb onto the polar face of ZnO[38] and the crystal growth rates of different ZnO facets are sensitive to variations in concentrations. The large quantity agglomerates maintains the crystal growth of ZnO by providing a sufficient supply of agglomerates. The constant crystal growth rates of ZnO result in the formation of ZnO nanorods with the uniform diameter from the bottom to top as shown in Fig. 6b-i. While in solutions treated in T1 way and T2 way, some octahedron combinations in agglomerates transfer to tetrahedron combinations as marked by the black dash lines in Fig. 6a-ii and Fig. 6a-iii,. Besides, the sizes of agglomerates are also enlarged by external force driving combinations of atoms onto agglomerates. As the concentrations of these building blocks decrease with their sizes, the crystal growth rates of ZnO declined in solutions with T1 and T2 treatments. Because of the anisotropic characteristic of ZnO, the growth rates of ZnO nonpolar facets are restrained greatly compared with polar surfaces. Thus, pyramidal-like structure, as shown in Fig. 6b-ii, is achieved by anisotropic growth of ZnO along the <0001> direction[18]. The rod-on-nanorod structure of ZnO in Fig. 6b-iii results from the abrupt declination in the amount of the large size agglomerates generated in solution treated in T2 way. The larger coaxial-cable ZnO nanostructure in Fig. 6b-iv formed with higher concentrations follows the same growth mechanism. Increase in the size of the sample in Fig. 6b-iv can be ascribed to the enlargement in the size of agglomerates in Fig. 6a-iii, which promote the crystal growth of ZnO in both longitude and latitude directions. With the consumption of agglomerates, the difference of growth rates between the polar and nonpolar faces are further enlarged by further prolonging the reaction duration from 3 h to 4.75 h. As shown in Fig. 6b-v, pencil-like ZnO nanostructure can also be formed by the predominant crystal growth of ZnO along c axis. It is also worth to point out that increase in the size of agglomerates also facilitate the homogeneous nucleation process,[39] which explains the low density of ZnO in Fig. 2c.

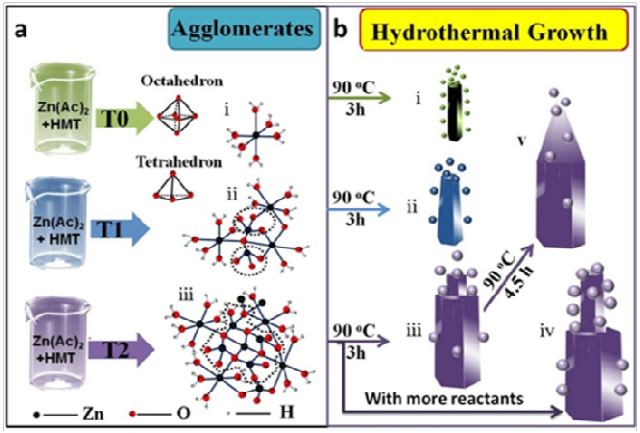

Fig. 6 Schematic diagrams for crystal growth of different ZnO in disturbed solutions; The green, blue and purple solid spheres in Fig. 6b represents agglomerates formed in solutions with T0, T1 and T2 treatments, respectively.

Conclusions

Tunable growth of different ZnO nanostructures is achieved by hydrothermal method with disturbed solutions. The reaction solution is composed of zinc acetate dihydrate and hexamine, no other surfactants are introduced. By exerting stirring or aging processes to solutions, agglomerates with different structures are formed and serve as building blocks for hydrothermal growth of ZnO. In a sealed solution, the concentration of agglomerate shall be in reverse relationship with its size. Thus, controllable growth of ZnO can be designed from the dynamic view by tuning the size of different agglomerates through stirring and aging pretreatments to solutions. Larger agglomerates with low amounts, which are the key factor for the formation of coaxial-cable like ZnO nanostructures, are formed by treating the solution in T1 or T2 way. Particularly, by prolonging the growth duration to 4.75 h, ZnO nanopencils with sharp tips can be fabricated with solution treated in T2 way. The XRD and PL results indicate that the as-synthesized ZnO nanopencils are with high crystalline and optical properties. Most importantly, by XAFS characterization on variations in the structure of agglomerates, this fundamental research provides an atomic mechanism for the formation of different ZnO nanostructures and illustrates a new concept for fabrications of novel and useful nanomaterials as well.

ACKNOWLEDGMENTS

This work is supported by National Science Foundation (No. 61306014); The Fundamental Research Funds for the Central Universities (Grant No. HIT. NSRIF. 2013009); Harbin Special Fund for Creative Talents in Science and Technology (No. 2012RFLXG029); Key Laboratory of Nanodevices and Applications, Suzhou Institute of Nano-Tech and Nano-Bionics, Chinese Academy of Sciences (No. 13ZS01); Open Project Program of Key Laboratory for Photonic and Electric Bandgap Materials, Ministry of Education, Harbin Normal University, (No. PEBM201302).

Notes and references

[a] School of Materials Science and Engineering, Harbin Institute of Technology, Harbin 150001, P. R. China; E-mail: shujiejiao@gmail.com; gaoshiyong@hit.edu.cn
[b] Key Laboratory for Photonic and Electric Bandgap Materials, Ministry of Education, Harbin Normal University, Harbin, 150025, P. R. China
[c] Key Laboratory of Nanodevices and Applications, Suzhou Institute of Nano-Tech and Nano-Bionics, Chinese Academy of Sciences, Suzhou, 215123 , P. R. China

1 A. Gokarna, J-H Kim, F. Leroy, G. Patriarche, P. Roussel, Z. Bougrioua, C. Rodriguez, E. Dogheche and Y-H Cho, *J. Lumin.*, 2013, **144**, 234.
2 S. Bai, L. Chen, S. Chen, R. Luo, D. Li, A. Chen and C. C. Liu, *Sens. Actuators B: Chemical*, 2014, **190**,760.
3 S, Kim, M, Kim, T. Kim, H. Baik and K. Lee, *CrystEngCommon*, 2013, **15**, 2601.
4 Y. K. Su, S. M. Peng, L. W. Ji, C. Z. Wu, W. B. Cheng and C. H. Liu, *Langmuir*, 2010, **26**, 603.
5 G. Shen, Y. Bando, B. D. Liu, D. Golberg and C-J. Lee, *Adv. Funct. Mater.*, 2006, **16**, 410.
6 C-Y Liu, Y-H Lai, H-S Wen, J-G Chen, C-W Kung, R. Vittal, and K-C Ho, *Energy Environ. Sci.*, 2011, **4**, 3448.
7 B. Liu, J. Xu, S. Ran, Z. Wang, D. Chen and G. Shen, *CrystEngComm*, 2012, **14**,4582.
8 (a) S. S. Warule, N. S. Chaudhari, J. D. Ambekar, B. B. Kale and M. A. More, *Appl. Mater. Inter.*, 2011, **3**, 3454; (b) S. Venkatachalam, H. Hayashi, T. Ebina, T. Nakamura, Y. Wakui and H. Nanjo, *J. Colloid Interface Sci.*, 2013, **395**, 64.
9 (a) Y. Liu, Y. Xie, J. Chen, J. Liu and C. Gao, *J. Am. Cream. Soc.*, 2011, **94**, 4387; (b) Y-H Sung, W-P Liao, D-W, Chen, C-T Wu, G-J Chang and J-J Wu, *Adv. Funct. Mater.*, 2012, **22**, 3808.
10 D. Nakamura, T. Shimogaki, S. Nakao, K. Ha.rada, Y. Muraoka, H. Ikenoue and T. Okada, *J. Phys. D: Appl. Phys.,* 2014, **47**, 22.
11 P. Sundara Venkatesh, C. L. Dong, C. L. Chen, W. F. Pong, K. Asokan and K. Jeganathan, *Mater. Lett.*, 2014, **116**, 206.
12 H. Wang and Y. Lian, *J. Alloy. Compd.,* 2014, **594**, 141.
13 F. Z. Haque and M. R. Parra, *Ultra Engineer*, 2012, **1**, 01.
14 H. L. Li, S. J. Jiao, H. T. Li and L. Li, *J Mater Sci: Mater Electron,* 2014, **25**, 2569.
15 B. Ikizler and S. M. Peker, *Thin Solid Films*, 2014, **558**, 149.
C-H Choi, Y-W Su and C-H Chang, *CrystEngComm*, 2013, **15**, 3226.
17 C-Y Kuo, R-U Ko, Y-C Tu, Y-k Lin, T-h Lin and S-J Wang, *Cryst. Growth. Des.*, 2012, **12**, 3849.
18 H. L. Li, S. J. Jiao, S. S. Bai, H. T. Li, S. Y. Gao, J. Z. Wang, Q. J. Yu, F. Y. Guo and L. C. Zhao, *Phys. Status Solidi (a)*, 2014, **211**, 3595.
19 L. L. Yang, Q. X. Zhao, M. Willander and J. H. Yang, *J. Cryst. Growth*, 2009, **311**, 1046.
20 Z. Q. Zhang and J. Mu, *J. Colloid Interface Sci.*, 2007, **307**, 79.
21 L. Kumari and W. Z. Li, *Cryst. Res. Technol.*, 2010, **45**, 311.
22 S. Ilican, *J. Alloys Compd.*, 2013, **553**, 225.
23 D. Polsongkram, P. Chamninok, S. Pukird, L. Chow, O. Lupan, G. Chai, H. Khallaf, S. Park and A. Schulte, *Physica B*, 2008, **403**, 3713.

24 K. O. Choi, S. H. Yoon, W-S Kim, K-H Lee, C-M Yang, J. H. Han, C. J. Kang, Y. J. Choi and T-S Yoon, *Phys. status solidi (a*), 2013, **210**, 1448.

25 S. S. Warule, Nilima S. Chaudhari, Jalindar D. Ambekar, B. B. Kale and M. A. More, *Appl. Mater. Interfaces*, 2011, **3**, 3454.

26 Y. X. Liu, Y. Z. Xie, J. T. Chen, J. Liu, C. Gao, C. Yun, B. Lu and E. Xie, *J. Am. Ceram. Soc.*, 2011, **94**, 4387.

27 H. B. Zeng, G. T. Duan, Y. Li, S. K. Yang, X. X. Xu and W. P. Cai, *Adv. Funct. Mater.*, 2010, **20**, 561.

28 B. G. Wang, E. W. Shi and W. Z. Zhong, *Cryst. Res.Technol.*, 1997, **32**, 659.

29 D. Polsongkram, P. Chamninok, S. Pukird, L. Chow, O. Lupan, G. Chai, H. Khallaf, S. Park and A. Schulte, *PhysicaB: Condensed Matter*, 2008, **403**, 3713.

30 Y. Sun, D. J. Riley and M. N. R. Ashfold, *J. Phys. Chem. B*, 2006, **110**, 15186.

31 Q. W. Li, J. M. Bian, J. C. Sun, J. W. Wang, Y. M. Luo, K. T. Sun and D. Q. Yu, *Appl. Surf. Sci.*, 2010, **256**, 1698.

32 S. Baruah and J. Dutta, *J. Cryst. Growth*, 2009, **311**, 2549.

33 A. Kawska, P. Duchstein, O. Hochrein and D. Zahn, *Nano Lett.* 2008, **8**, 2336.

34 S-Q Wei, Z-H Sun, Z-Y Pan, X-Y Zhang, W-S Yan, W-J. Zhong, *J. Nucl. Sci. Technol.*, 2006, **17**, 370.

35 E. A. Stern, M. Newville, B. Ravel, Y. Yacoby and D. Haskel, *Physica B*, 1995, **208&209**, 117.

36 (a) Y. S. Kim and Y. S. Won, *Bull. Korean Chem. Soc.*, 2009, **30**, 1573; (b) G. Apai and J. F. Hamilton, *Phy. Rev. Lett.,*1979, **43**, 165.

37 D. R. Roberts, R. G. Ford and D. L. Sparks, *J. Colloid Interface Sci.*, 2003, **263**, 364.

38 M. Wang, Y. Zhou, Y. Zhang, S. H. Hahn and E. J. Kim, *CrystEngComm*, 2011, **13**, 6024.

39 S. Xu and Z. L. Wang, *Nano Res.*, 2011, **4**, 1013.

Cite this: DOI: 10.1039/c0xx00000x

www.rsc.org/xxxxxx

ARTICLE TYPE

Dynamically controlled synthesis of different ZnO nanostructures by surfactant-free hydrothermal method

Haili Li,[a] Shujie Jiao,*[a,b,c] Shiyong Gao,*[a] Hongtao Li[a] and Lin Li[b]

Received (in XXX, XXX) Xth XXXXXXXXX 20XX, Accepted Xth XXXXXXXXX 20XX

DOI: 10.1039/b000000x

Textual and graphical abstract

Dynamically controlled hydrothermal growth of different ZnO nanostructures in physical disturbances-treated solutions and atomic analysis based on XAFS characterization.